

The logo for EPJ B features a dark blue background with a red and orange abstract pattern on the left side. The text "EPJ B" is written in a white, serif font.

EPJ B

www.epj.org

Condensed Matter
and Complex Systems

Eur. Phys. J. B **66**, 235–238 (2008)

DOI: 10.1140/epjb/e2008-00394-3

Analytical calculation of eigen-energies for lens-shaped quantum dot with finite barriers

A.H. Rodríguez and H.Y. Ramírez



Analytical calculation of eigen-energies for lens-shaped quantum dot with finite barriers

A.H. Rodríguez^{1,a} and H.Y. Ramírez^{2,3}

¹ Universidad Autónoma de la Ciudad de México (UACM), Calzada Ermita Iztapalapa s/n Col. Lomas de Zaragoza, C.P. 09620, Iztapalapa, México D.F., México

² Physics Department, Universidad de Los Andes, Carrera 1. No. 18A-10, Bogotá, Colombia

³ Electrophysics Department, National Chiao Tung University, 1001 Ta Hsueh Road, Hsinchu R.O.C., Taiwan

Received 8 July 2008

Published online 24 October 2008 – © EDP Sciences, Società Italiana di Fisica, Springer-Verlag 2008

Abstract. The bound states of a particle in a lens-shaped quantum dot with finite confinement potential are obtained in the envelope function approximation. The quantum dot has circular base with radius a and maximum cap height b , and the effective mass of the particle is considered different inside and outside the dot. A 2D Fourier expansion is used in a semi-sphere domain with infinite walls which contains the geometry of the original potential. Electron energies for different values of lens deformation b/a , lens radius a and barrier height V_0 are calculated. In the very high confinement potential limit, the results for the infinite barrier case are recovered.

PACS. 02.30.Nw Fourier analysis – 73.22.-f Electronic structure of nanoscale materials: clusters, nanoparticles, nanotubes, and nanocrystals – 73.22.Dj Single particle states

1 Introduction

The carrier confinement within small regions such as quantum wells [1], quantum wires [2] and quantum dots [3,4] are of a great importance when in describing transport phenomena, electrical and optical properties of these “man-made” systems. Different geometries have been considered (pyramids [5–9], quantum disks [10], spherical quantum dots [11–13], quantum lenses [14–19] and even an arbitrary geometry [20]). Due to complex realistic geometries and boundary conditions to include the effects of the surrounding media, it is not possible in general to find analytical solutions using common standard procedures. As a first approximation, impenetrable barriers are often considered since it simplifies the mathematical problem. Nevertheless, the finite value of the potential barrier could be a fundamental parameter when considering different external potentials or when including others physical effect, such as the presence of a hydrostatic pressure in a quantum dot [21].

When including the finite barrier, different approaches have been used. Bound states in rectangular cross-section quantum wires as products of eigenstates of 1D problems with a finite barrier in each direction were found in reference [22]. The energy levels are then corrected by the first-order perturbation-theory. It was shown that the method

is suitable for rectangles with sufficiently large linear dimensions. The same idea was previously applied in [23] to calculate the electronic states in cylindrical quantum dots of semiconductors. A 2D Fourier expansion has been used in [24] to find the electronic states in InGaAs/InP quantum well-wires structures and in self-assembled InAs pyramidal quantum dots [25].

Likewise, previous theoretical studies in self-assembled quantum dots with lens shape considered infinite wall potential [26–28]. The aim of the present work is to develop a model which allows the analytical calculations of the electronic levels in self-assembled quantum dots with lens shape including a finite barrier potential. The obtained results are compared with those from considering infinite barrier model and analysis is done establishing the cases where the later represents a good approximation. The solution of the problem is also found using numerical calculations for comparing with the analytical results. Finally, some conclusion are outlined.

2 Model for finite potential

The eigenvalue problem of the Schrödinger equation in a 3D lens shape with infinite barriers in the effective mass approximation has been solved elsewhere [26]. In our case, the problem for a finite barrier will be modeled including a lens shape well potential with height V_0 in a

^a e-mail: arezky@gmail.com

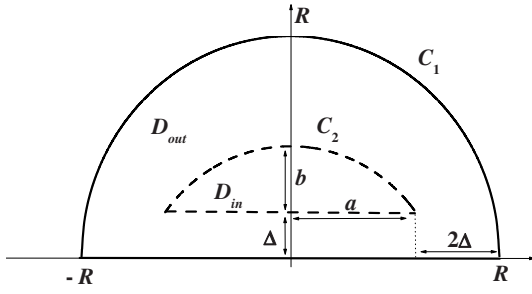


Fig. 1. Transversal section of a 3D finite lens-well D_{in} with barrier height V_o and contour C_2 inside an infinite semispherical-well with contour C_1 . Contour C_1 and C_2 are separated a distance equal or greater than Δ along the perpendicular axis.

hard-walls semi-spherical region as shown in Figure 1. The semi-spherical region is divided in two regions, D_{out} with potential V_o and region D_{in} where it is zero. We will consider a different value of effective mass for the particle in each region. The solution of the problem given by the lens with finite barrier in an infinite surrounding medium can be obtained by minimizing the effect of the external boundary C_1 over the wavefunction of the corresponding energy level under study. This can be achieved by taking a high enough value of the distance Δ . The equation for the whole region D is given by:

$$-\frac{\hbar^2}{2} \nabla \left(\frac{1}{m^*(r, \theta, \phi)} \nabla \Psi \right) + V(r, \theta, \phi) \Psi = E \Psi, \quad (r, \theta, \phi) \in D = D_{in} + D_{out} \quad (1)$$

where

$$V(r, \theta, \phi) = \begin{cases} 0; & (r, \theta, \phi) \in D_{in} \\ V_o; & (r, \theta, \phi) \in D_{out} \end{cases} \quad (2)$$

and

$$m^*(r, \theta, \phi) = \begin{cases} m_{in}^*; & (r, \theta, \phi) \in D_{in} \\ m_{out}^*; & (r, \theta, \phi) \in D_{out}. \end{cases} \quad (3)$$

The analytical solution of equation (1) is sought in the form of an expansion

$$\Psi = \sum_i C_i \Psi_i^{(o)} \quad (4)$$

where the set of functions $\{\Psi_i^{(o)}\}$ is a complete set of functions in the 3D domain D given by the semi-sphere. Its explicit representation can be found in [26], where a diagonalization procedure was implemented to obtain the electron states. With such conditions, the functions Ψ satisfy the boundary condition of infinite barrier in the contour C_1 because the set of functions $\{\Psi_i^{(o)}\}$ does. On the other hand, equation (1) and the corresponding solution given by equation (4) are given in the whole domain D . It guarantees that the matching conditions at

the contour C_2 are also satisfied, but only at those points where the derivative of the wavefunction is well-defined. This does not occur at the corner and, generally speaking, the problem is then not well-defined. Then, the obtained eigenvalues constitute only an estimation of the real problem but this solution constitute a better estimation of the eigenvalues when the finite barrier is included. This treatment has been applied in [23] for a cylindrical domain and in [29] for a rectangle, but not explicit analysis was done in the fulfillment of the matching conditions between the internal and the external domain.

Equation (1) can be rewritten as:

$$-\nabla^2 \Psi - \sigma(r, \theta, \phi) \nabla \left(\frac{1}{\sigma(r, \theta, \phi)} \right) \nabla \Psi + \mathcal{V}(r, \theta, \phi) \sigma(r, \theta, \phi) \Psi = \lambda \sigma(r, \theta, \phi) \Psi \quad (5)$$

where $\sigma(r, \theta, \phi) = 1$ and $\mathcal{V}(r, \theta, \phi) = 0$ in the internal region D_{in} and $\sigma(r, \theta, \phi) = \sigma = m_{out}^*/m_{in}^*$ and $\mathcal{V}(r, \theta, \phi) = \mathcal{V}_o = V_o/E_o$ in the external domain D_{out} . The eigenvalue is given now by $\lambda = E/E_o$ where $E_o = \hbar^2/2m_{in}^*R^2$ is the unit of energy.

From equations (5) and (4) it is obtained the matrix representation of the problem

$$\sum_i C_i \left\{ \lambda_i^{(o)} \delta_{ij} - \mathcal{C}(i, j) + \mathcal{A}(i, j) - \lambda \mathcal{B}(i, j) \right\} = 0 \quad (6)$$

where $\lambda_i^{(o)}$ are the corresponding eigenvalues of the set of functions $\{\Psi_i^{(o)}\}$. The matrix

$$\mathcal{C}(i, j) = \left\langle \Psi_j^{(o)} \left| \sigma \nabla \left(\frac{1}{\sigma} \right) \nabla \Psi_i^{(o)} \right\rangle_D \quad (7)$$

is equal to zero because of the finite discontinuity of $\sigma(r, \theta, \phi)$, and

$$\begin{aligned} \mathcal{A}(i, j) &= \left\langle \Psi_j^{(o)} \left| \mathcal{V}(r, \theta, \phi) \sigma(r, \theta, \phi) \Psi_i^{(o)} \right\rangle_D \\ &= \mathcal{V}_o \sigma \left[\delta_{i,j} - \left\langle \Psi_j^{(o)} \left| \Psi_i^{(o)} \right\rangle_{D_{in}} \right] \end{aligned} \quad (8)$$

$$\begin{aligned} \mathcal{B}(i, j) &= \left\langle \Psi_j^{(o)} \left| \sigma(r, \theta, \phi) \Psi_i^{(o)} \right\rangle_D \\ &= \left\langle \Psi_j^{(o)} \left| \Psi_i^{(o)} \right\rangle_{D_{in}} + \sigma \left[\delta_{i,j} - \left\langle \Psi_j^{(o)} \left| \Psi_i^{(o)} \right\rangle_{D_{in}} \right] \end{aligned} \quad (9)$$

where $\langle \rangle_{D_{in}}$ means an integration over the internal domain D_{in} .

According to the axial symmetry, the Hilbert space of the problem given by equation (6) is separated in different subspaces, each one characterized by a quantum number m . The first five eigenvalues λ for $b/a = 0.51$ as a function of the external potential \mathcal{V}_o are shown in Figure 2. Each one is labeled by a couple of indexes (N, m) meaning the N th energy level with axial quantum number m . It is used $\sigma = m_{out}^*/m_{in}^* = 3.5$ which is the ratio between the values of the effective masses in an InAs/GaAs

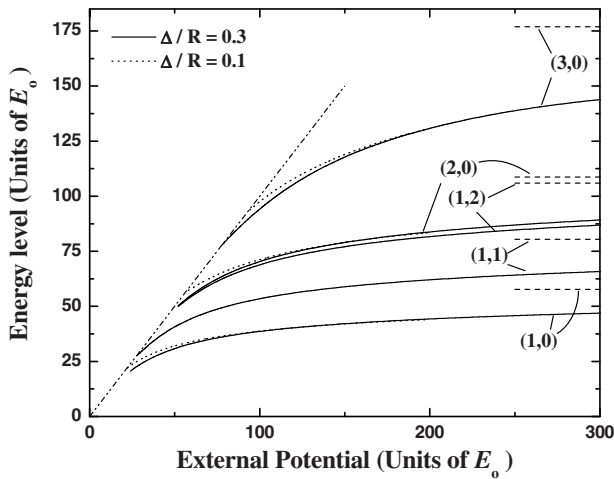


Fig. 2. First five energy levels for a lens-shaped quantum dot with $b/a = 0.51$ as a function of the external potential barrier \mathcal{V}_o in dimensionless quantities. The calculation is done taking $\Delta/R = 0.3$ (solid lines) and $\Delta/R = 0.1$ (dotted lines). In both cases it is used $\sigma = 3.5$. Dashed lines represent the infinite barrier case [26] while dash-dot-dot is the line where the energy value is equal to the potential value.

quantum dot material [21]. It can be seen that, as the external potential increases, also increase the energy levels approaching asymptotically to the corresponding values of the infinite potential case which are shown horizontally in dashed lines [26]. For a given value of the potential barrier, the energy values for the lower levels are closer to the corresponding value taken the barrier as infinite than those for higher levels, as expected. At the same time, as higher the level, higher the percent of the wavefunction located at region D_{out} and stronger the influence of the artificial boundary C_1 . This influence is also stronger for lower values of Δ/R . This effects can be seen in Figure 2 when comparing the solid lines, calculated by using $\Delta/R = 0.3$, with the dotted lines, calculated by using $\Delta/R = 0.1$ (only for levels with $m = 0$). However, at those values of the potential barrier where the solution is independent of the parameter Δ/R , the solution can be taken as independent of the boundary C_1 and hence, as a good approximation for the finite barrier case in an infinite surrounding medium. Dash-dot-dot line represents the points where the energy value is equal to the potential value.

In order to study a particular quantum dot material, two different quantum lens configuration of InAs/GaAs have been considered. In Figure 3 the first five electronic levels are shown as a function of the lens radius, where a 500×500 matrix was used in the diagonalization procedure. The material parameters used here for the calculation are the same as in [21].

In general, the values of the energy levels decrease for increasing values of the radius. As shown in Figure 3a, for $b/a = 0.91$ and according to the levels shown, the infinite barrier model is a good approximation for radius of the order of 20 nm or higher. Nevertheless, as seen in Figure 3b, for lower values of b/a it is necessary to include the finite

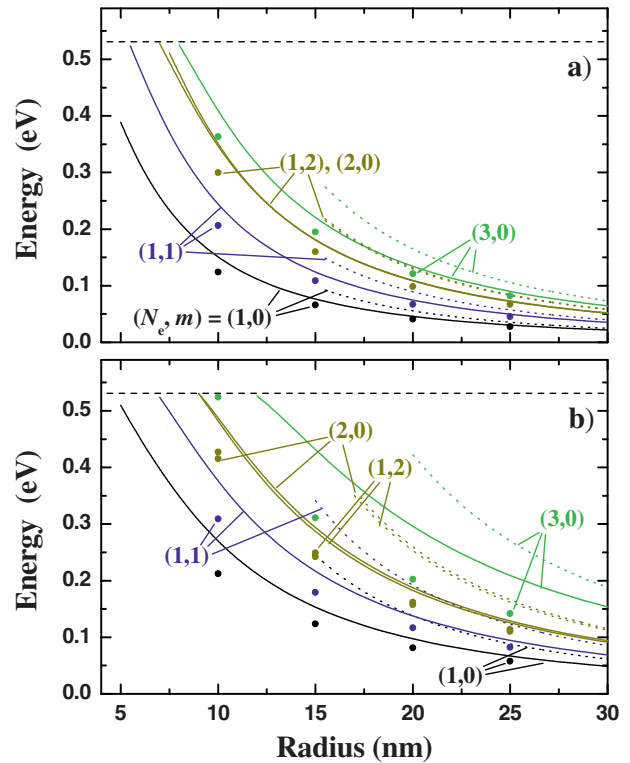


Fig. 3. First five electronic levels for an InAs/GaAs quantum lens as a function of the lens radius. (a) $b/a = 0.91$, (b) $b/a = 0.51$. The calculation is done taking $\Delta/R = 0.3$ (solid lines). Results from the infinite barrier model are also plotted for comparison (dotted lines). As a reference, the value for the confinement potential used ($V_c = 0.531$ eV) is shown by dashed line in both panels. Filled dots correspond to numerical calculations.

barrier effects to get better approximations of the energy levels distribution for all the values of the radius shown.

As an intend of verifying the obtained results, numerical calculations were carried out solving directly the BenDaniel-Duke equation of the system, calculating the eigenvalues by using the finite elements technique through programs for Comsol application, as used in previous works [30,31]. The corresponding results are shown by filled dots in Figure 3, calculated with the same material and geometrical parameters as those used in the analytical curves. Although qualitatively the behavior of the analytical and numerical results are consistent, since the quantitative point of view the numerically obtained values have always lower values than those represented by the solid and the dotted lines. Furthermore, the tree models coincide for higher enough values of the dot radius, but its results become different when the radius decreases. The result obtained is mainly due to the presence of the frontier C_1 (at the analytical calculation) whose effects become important for smaller dots because of the increasing of the energy values and correspondingly, the wavefunction has higher percent outside the lens domain given by D_{in} in Figure 1. In the same way, the necessary basic truncation introduce an error which becomes important for smaller

dots and, as found in [26], the accuracy of the analytical method requires bigger matrices for larger lens deformation (smaller values of b/a), which is in agreement with the comparison of panels a) and b) from Figure 3.

3 Conclusions

In the present work the results from [26,27] have been generalized to evaluate the electronic energies in self-assembled quantum dots with lens shape geometry taking into account the finite barrier height. The results obtained by the present model was compared with the values obtained when considering the potential barrier as infinite and with a numerical calculation procedure. It was established the range of values for the potential barrier, lens deformation b/a and lens radius a where all the models produce similar results. It was also argue the reasons for its different energy values obtained for smaller dots and for stronger lens deformations. The present model can be applied to study analytically the electronic properties of a self-assembled quantum dots with lens shape under the presence of external potentials where it could be important to consider the actual values of the finite barrier.

The authors thank many valuable discussions with Dr. C. Trallero-Giner.

References

1. C. Trallero-Giner, J. López-Gondar, *Physica B* **138**, 287 (1986)
2. C.A.T. Herrero, C.T. Giner, S.E. Ulloa, R.P. Alvarez, *Phys. Rev. E* **64**, 056237 (2001)
3. L. Jacak, P. Hawrylak, A. Wojs, *Quantum dots* (Springer-Verlag, Berlin, 1998)
4. D. Bimberg, M. Grundmann, N.N. Ledentsov, *The quantum dot heterostructures* (Wiley, Chichester, 1999)
5. M.A. Cusack, P.R. Briddon, M. Jaros, *Phys. Rev. B* **54**, R2300 (1996)
6. M.A. Cusack, P.R. Briddon, M. Jaros, *Phys. Rev. B* **56**, 4047 (1997)
7. M. Grundmann, O. Stier, D. Bimberg, *Phys. Rev. B* **52**, 11969 (1995)
8. C. Pryor, *Phys. Rev. B* **57**, 7190 (1998)
9. O. Stier, M. Grundmann, D. Bimberg, *Phys. Rev. B* **59**, 5688 (1999)
10. E. Menéndez-Proupin, C. Trallero-Giner, S.E. Ulloa, *Phys. Rev. B* **60**, 16747 (1999)
11. J.L. Marín, R. Riera, S.A. Cruz, *J. Phys.: Condens. Matter* **10**, 1349 (1998)
12. E. Menéndez, C. Trallero-Giner, M. Cardona, *Phys. Stat. Sol. (b)* **199**, 81 (1997)
13. T. Uozumi et al., *Phys. Rev. B* **59**, 9826 (1999)
14. A. Forchel et al., *Semicond. Sci. Technol.* **11**, 1529 (1996)
15. I. Hapke-Wurst et al., *Semicond. Sci. Technol.* **14**, L41 (1999)
16. J.H. Zhu, K. Brunner, G. Abstreiter, *Appl. Phys. Lett.* **72**, 424 (1998)
17. J. Zou, X.Z. Liao, D.J.H. Cockayne, R. Leon, *Phys. Rev. B* **59**, 12279 (1999)
18. J. Even, C. Cornet, S. Loualiche, *Physica E* **28**, 514 (2005)
19. C. Cornet, J. Even, S. Loualiche, *Phys. Lett. A* **344**, 457 (2005)
20. A.A. Kiselev, K.W. Kim, M.A. Stroschio, *Phys. Rev. B* **60**, 7748 (1999)
21. C.A. Duque et al., *J. Phys.: Condens. Matter* **18**, 1877 (2006)
22. M. Califano, P. Harrison, *J. Appl. Phys.* **86**, 5054 (1999)
23. S.L. Goff, B. Stébé, *Phys. Rev. B* **47**, 1383 (1993)
24. D. Gershoni et al., *Appl. Phys. Lett.* **53**, 995 (1988)
25. M. Califano, P. Harrison, *J. Appl. Phys.* **88**, 5870 (2000)
26. A.H. Rodríguez, C.R. Handy, C. Trallero-Giner, *J. Phys.: Condens. Matter* **15**, 8465 (2003)
27. A.H. Rodríguez, C. Trallero-Giner, *J. Appl. Phys.* **95**, 6192 (2004)
28. A.H. Rodríguez, C. Trallero-Giner, M. Muñoz, M.C. Tamargo, *Phys. Rev. B* **72**, 045304 (2005)
29. A. Bruno-Alfonso (personal communication)
30. H.Y. Ramirez, A.S. Camacho, L.L.Y. Voon, *J. Phys.: Condens. Matter* **19**, 346216 (2007)
31. H.Y. Ramirez, A.S. Camacho, L.L.Y. Voon, *Nanotechnology* **17**, 1286 (2006)